Chiral dynamics in "rigid" and "soft" triaxial nuclei

Pengwei Zhao 赵鹏巍

Peking University

Outline

- Nuclear chirality with covariant density functional theory
- Chiral dynamics in triaxial nuclei: chiral precession
- Chiral dynamics in soft triaxial nuclei
- Summary

Nuclear spin-chirality

The aplanar (3D-) rotation of a triaxial nucleus could present chiral geometry.

Frauendorf and Meng, Nucl. Phys. A **617**, 131 (1997)

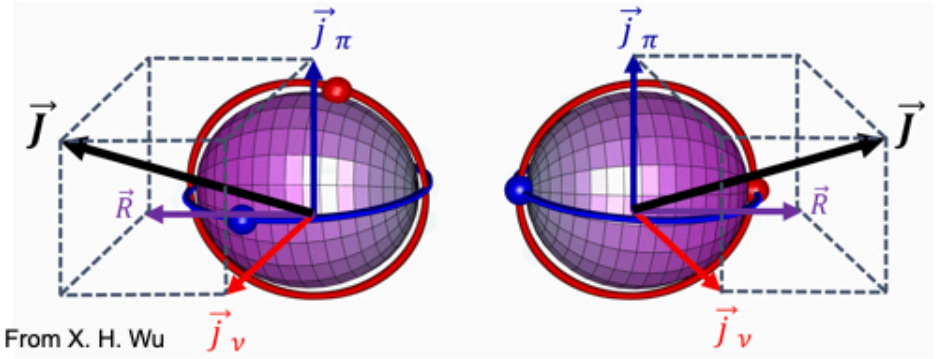

Left-handed $|\mathcal{L}\rangle$ Right-handed $|\mathcal{R}\rangle$

Intrinsic frame:

Chiral Symmetry breaking

$$\hat{\chi} = \hat{T}\hat{R}_y(\pi)$$

$$\hat{\chi}\,|\mathcal{L}\rangle = |\mathcal{R}\rangle \qquad \hat{\chi}\,|\mathcal{R}\rangle = |\mathcal{L}\rangle$$

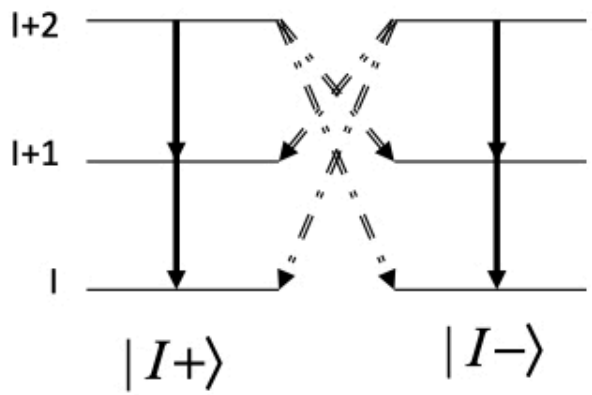

Lab. frame:

Chiral Symmetry restoration

$$|I+\rangle = \frac{1}{\sqrt{2}}(|\mathcal{L}\rangle) + |\mathcal{R}\rangle)$$

$$|I-\rangle = \frac{i}{\sqrt{2}}(|\mathcal{L}\rangle) - |\mathcal{R}\rangle)$$

Exp. signal: Two near degenerate ΔI =1 bands, called chiral doublet bands

Observed chiral nuclei

More than 45 candidate chiral nuclei have been reported in the A~80, 100, 130, and 190 mass regions, so far.

Xiong and Wang, At. Data Nucl. Data Tables, 2019, 125, 193-225

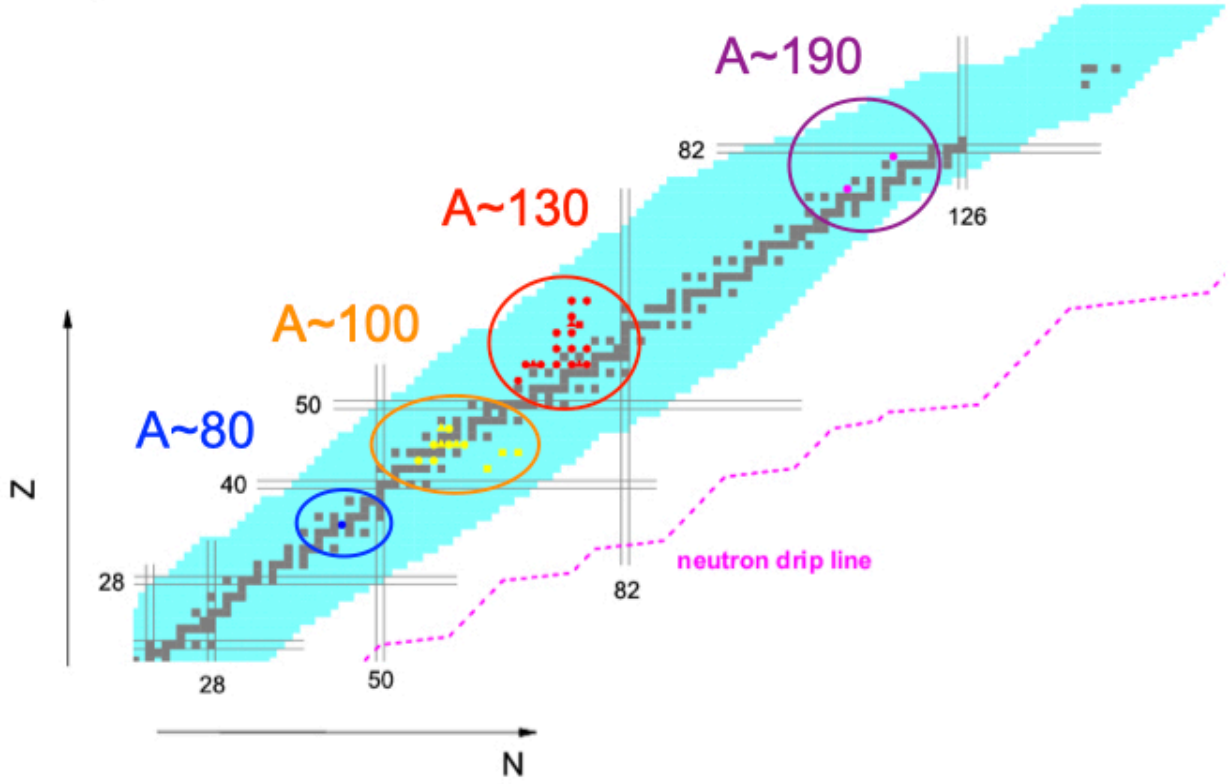

- ✓ **Triaxial deformation**: *less evident in the ground state*
- ✓ **Single-particle structure**: *isolate the role of specific orbitals*
- ✓ **Triaxial shape coexistence**: *a unique phenomenon of nuclear systems*

Theoretical tools for nuclear chirality

- **Particle Core Coupling**

  (lab frame, phenomenological, quantal, with quantum tunneling)

  - ✓ Triaxial Particle Rotor Model — Frauendorf and Meng NPA(1997); Koike PRL(2004), Qi PLB(2009)
  - ✓ Core-quasiparticle coupling model — Starosta PRC(2002); Koike PRC(2003)
  - ✓ Interacting Boson Fermion Fermion Model — Brant PRC (2004), PRC (2008), Tonev PRL(2006)

- **Tilted Axis Cranking Mean Field**

  (intrinsic frame, microscopic, semi-classical, no quantum tunneling)

  - ✓ Single-j model — Frauendorf and Meng NPA(1997)
  - ✓ Hybrid Woods-Saxon and Nilsson model — Dimitrov PRL(2000)
  - ✓ Non-relativistic Skyrme DFT — Olbratowski PRL(2004), PRC(2006)
  - ✓ **Covariant DFT** — PWZ PLB (2017)

- **Shell Model**

  - ✓ Pair Truncated Shell Model — Higashiyama, PRC(2005)
  - ✓ Projected Shell Model — Chen PRC (2017)

  ...

Tilted axis cranking CDFT

The cranking mean-field model has been very successful for rotations

Meson exchange version:

3-D Cranking: *Madokoro, Meng, Matsuzaki, Yamaji, PRC 62, 061301 (2000)*

2-D Cranking: *Peng, Meng, Ring, Zhang, PRC 78, 024313 (2008)*

Point-coupling version:

Simple and more suitable for systematic investigations

2-D Cranking: *PWZ, Zhang, Peng, Liang, Ring, Meng, PLB 699, 181 (2011)*

2-D Cranking + Pairing: *PWZ, Zhang, Meng, PRC 92, 034319 (2015)*

3-D Cranking: *PWZ, PLB 773, 1 (2017)*

3-D Cranking + Pairing: *in preparation*

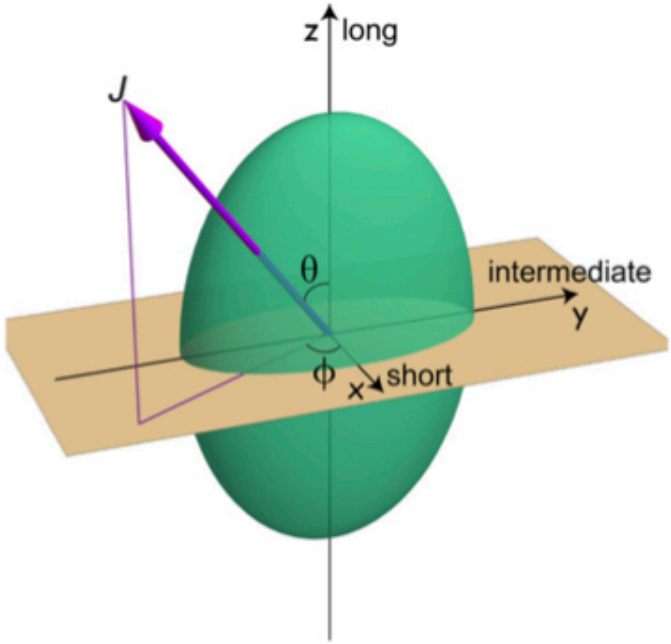

Self-consistent and microscopic investigations

✓ full account of polarization effects

✓ self-consistent treatment of the nuclear currents

✓ no additional parameter beyond a well-determined functional

Density functional theory

The many-body problem is mapped onto a one-body problem

Hohenberg-Kohn Theorem

The exact ground-state energy of a quantum mechanical many-body system is a universal functional of the local density.

$$E[\rho] = T[\rho] + U[\rho] + \int V(\mathbf{r})\rho(\mathbf{r})\,\mathrm{d}^3\mathbf{r}$$

Kohn-Sham DFT

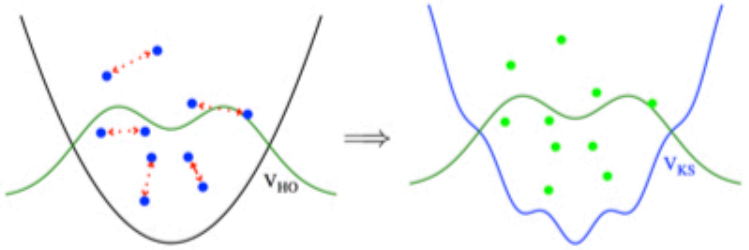

Figure from Drut PPNP 2010

$$T[\rho] \doteq \sum_{i=1}^{N} \left\langle \varphi_i \left| -\frac{\hbar^2}{2m}\nabla^2 \right| \varphi_i \right\rangle$$

$$E[\rho] \Rightarrow \boxed{\hat{h} = \frac{\delta E}{\delta \rho}} \Rightarrow \boxed{\hat{h}\varphi_i = \varepsilon_i \varphi_i} \Rightarrow \boxed{\rho = \sum_{i=1}^{A} |\varphi_i|^2}$$

The practical usefulness of the Kohn-Sham theory depends entirely on whether an Accurate Energy Density Functional can be found!

How many nuclei are bound?

http://nuclearmap.jcnp.org/index.html PC-PK1

Triaxial RHB

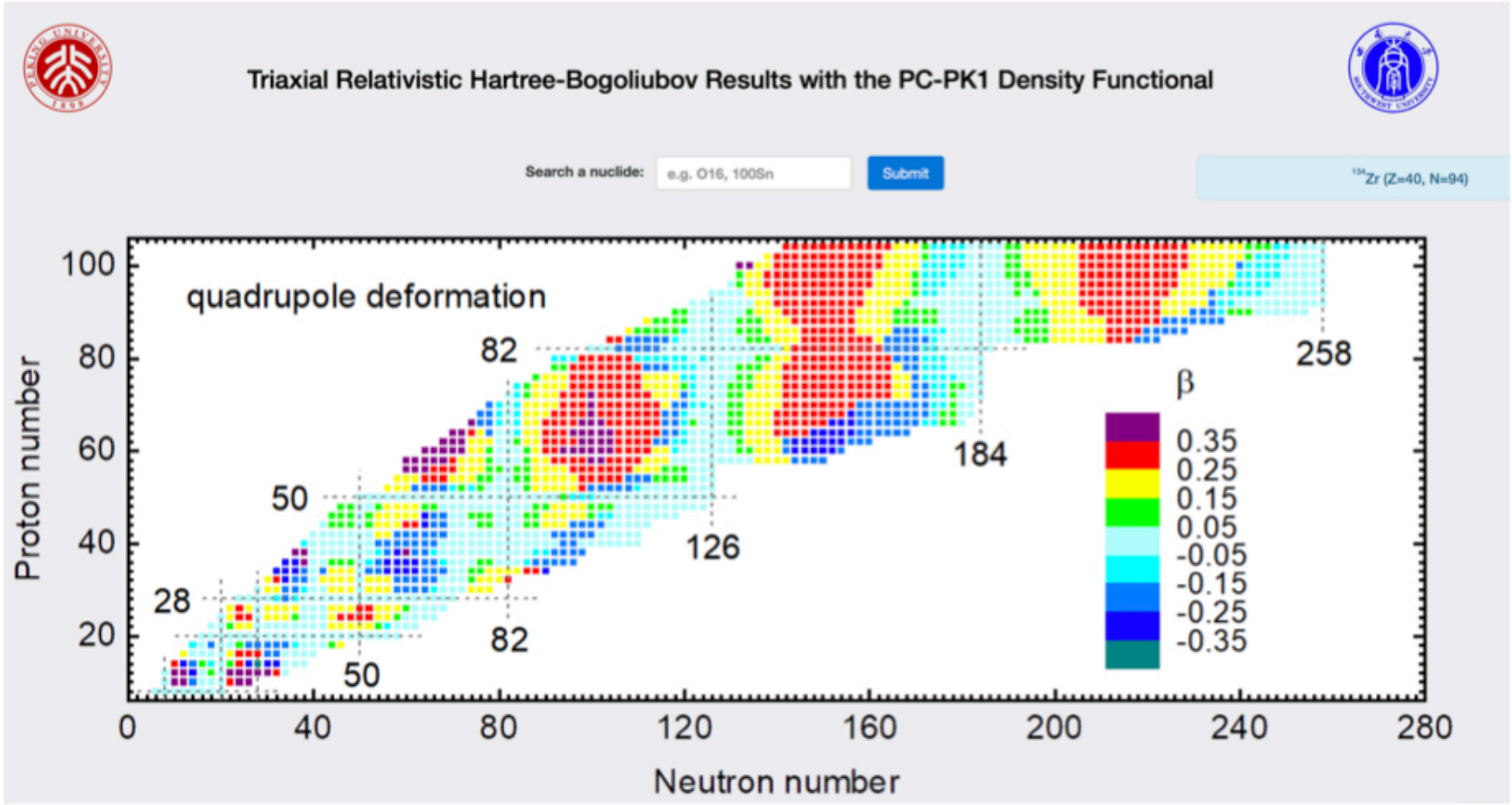

Yang, Wang, PWZ, Li, Phys. Rev. C 104, 054312 (2021)

Yang, PWZ, Li, Phys. Rev. C 107, 024308 (2023)

How many nuclei are bound?

http://nuclearmap.jcnp.org/index.html PC-PK1

Triaxial RHB

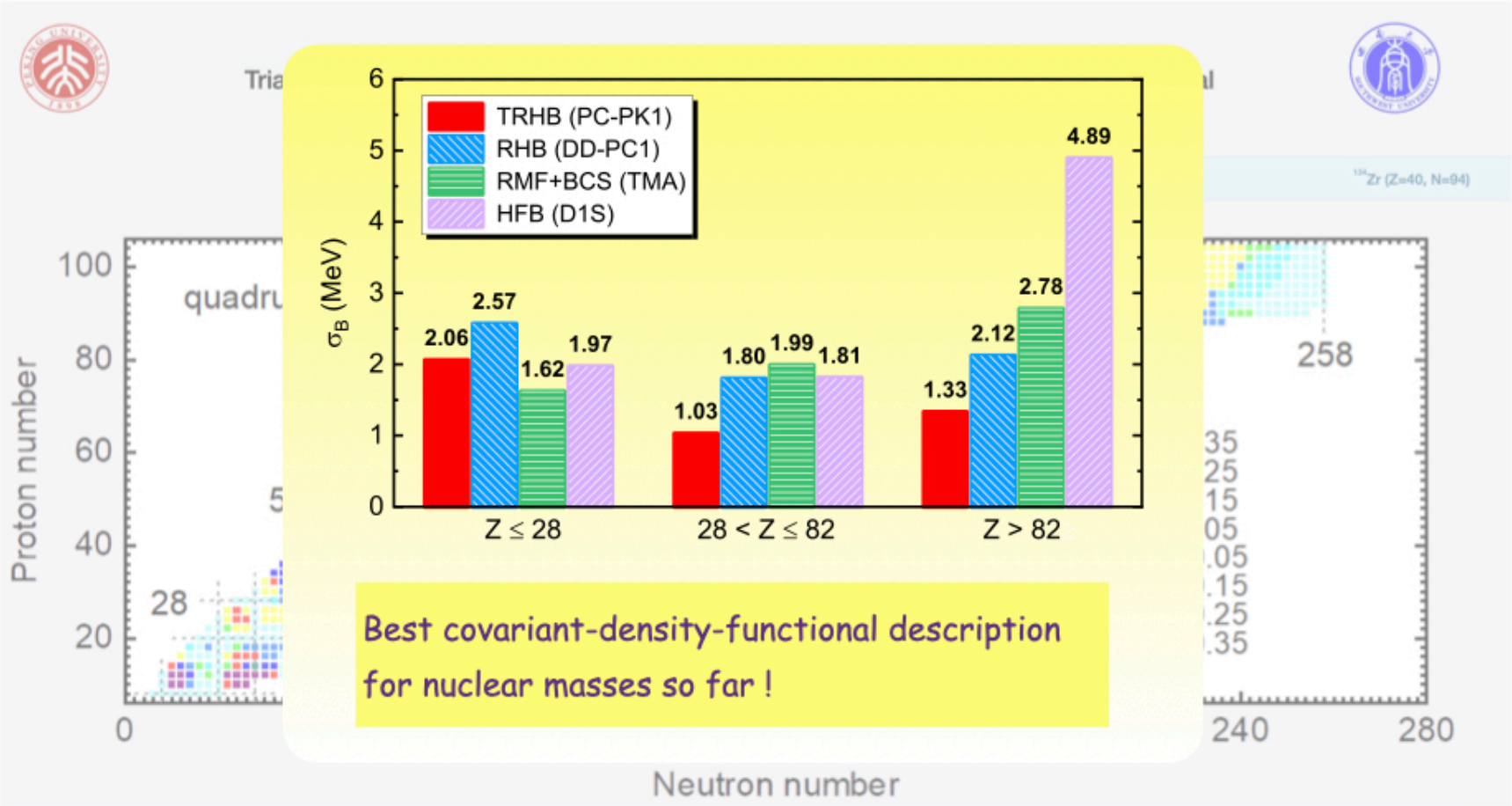

Yang, Wang, PWZ, Li, Phys. Rev. C 104, 054312 (2021)

Yang, PWZ, Li, Phys. Rev. C 107, 024308 (2023)

How many nuclei are bound?

http://nuclearmap.jcnp.org/index.html PC-PK1

Triaxial RHB

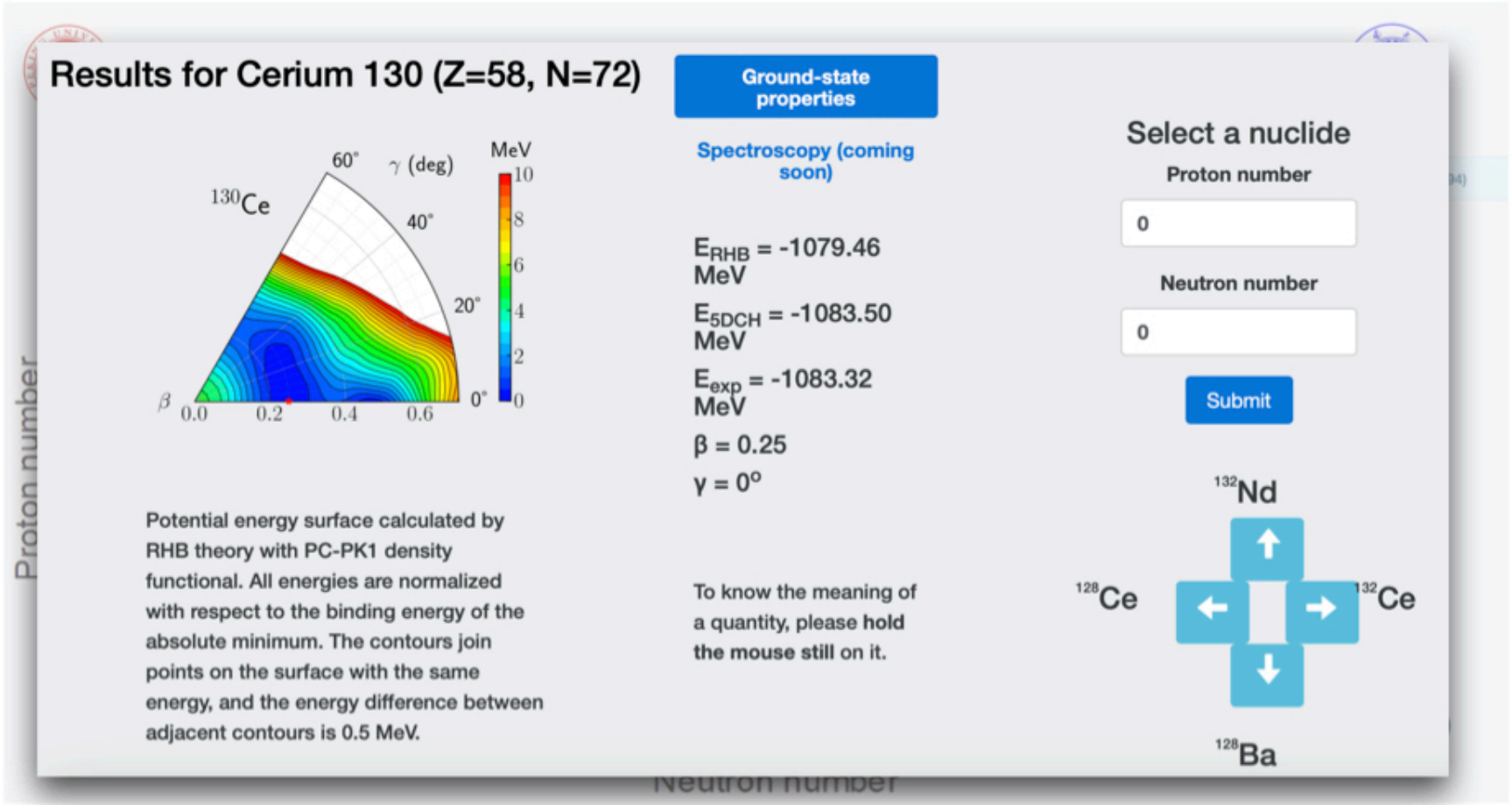

Yang, Wang, PWZ, Li, Phys. Rev. C 104, 054312 (2021)
Yang, PWZ, Li, Phys. Rev. C 107, 024308 (2023)

Cranking Relativistic Kohn-Sham Equation

Dirac Equation

$$\begin{pmatrix} m + V + S - \boldsymbol{\omega}\cdot\boldsymbol{J} & \boldsymbol{\sigma}\cdot\boldsymbol{p} - \boldsymbol{\sigma}\cdot\boldsymbol{V} \\ \boldsymbol{\sigma}\cdot\boldsymbol{p} - \boldsymbol{\sigma}\cdot\boldsymbol{V} & -m + V - S - \boldsymbol{\omega}\cdot\boldsymbol{J} \end{pmatrix} \begin{pmatrix} f \\ g \end{pmatrix} = \varepsilon \begin{pmatrix} f \\ g \end{pmatrix}$$

$$S(\boldsymbol{r}) = \alpha_S \rho_S + \beta_V \rho_S^2 + \gamma_V \rho_S^3 + \delta_S \Delta\rho_S$$

$$V(\boldsymbol{r}) = \alpha_V \rho_V + \gamma_V \rho_V^3 + \delta_V \Delta\rho_V + \tau_3 \alpha_{TV} \rho_{TV} + \tau_3 \delta_{TV} \Delta\rho_{TV} + e\frac{1-\tau_3}{2} A$$

$$\boldsymbol{V}(\boldsymbol{r}) = \alpha_V \boldsymbol{j}_V + \gamma_V \boldsymbol{j}_V^3 + \delta_V \Delta\boldsymbol{j}_V + \tau_3 \alpha_{TV} \boldsymbol{j}_{TV} + \tau_3 \delta_{TV} \Delta\boldsymbol{j}_{TV} + e\frac{1-\tau_3}{2} \boldsymbol{A}$$

Consistent treatment for time-odd fields from nuclear currents

PWZ, Zhang, Peng, Liang, Ring, Meng, PLB 699, 181 (2011)

PWZ PLB 773, 1 (2017)

Cranking Relativistic Kohn-Sham Equation

Dirac Equation Coriolis term Time-odd mean fields

$$\begin{pmatrix} m + V + S - \omega \cdot J & \boldsymbol{\sigma} \cdot \boldsymbol{p} - \boldsymbol{\sigma} \cdot \boldsymbol{V} \\ \boldsymbol{\sigma} \cdot \boldsymbol{p} - \boldsymbol{\sigma} \cdot \boldsymbol{V} & -m + V - S - \omega \cdot J \end{pmatrix} \begin{pmatrix} f \\ g \end{pmatrix} = \varepsilon \begin{pmatrix} f \\ g \end{pmatrix}$$

$$S(\boldsymbol{r}) = \alpha_S \rho_S + \beta_V \rho_S^2 + \gamma_V \rho_S^3 + \delta_S \Delta\rho_S$$

$$V(\boldsymbol{r}) = \alpha_V \rho_V + \gamma_V \rho_V^3 + \delta_V \Delta\rho_V + \tau_3 \alpha_{TV} \rho_{TV} + \tau_3 \delta_{TV} \Delta\rho_{TV} + e\frac{1-\tau_3}{2} A$$

$$\boldsymbol{V}(\boldsymbol{r}) = \alpha_V \boldsymbol{j}_V + \gamma_V \boldsymbol{j}_V^3 + \delta_V \Delta\boldsymbol{j}_V + \tau_3 \alpha_{TV} \boldsymbol{j}_{TV} + \tau_3 \delta_{TV} \Delta\boldsymbol{j}_{TV} + e\frac{1-\tau_3}{2} \boldsymbol{A}$$

Consistent treatment for time-odd fields from nuclear currents

PWZ, Zhang, Peng, Liang, Ring, Meng, PLB 699, 181 (2011)

PWZ PLB 773, 1 (2017)

Cranking Relativistic Kohn-Sham Equation

Dirac Equation Coriolis term Time-odd mean fields

$$\begin{pmatrix} m + V + S - \omega \cdot J & \boldsymbol{\sigma} \cdot \boldsymbol{p} - \boldsymbol{\sigma} \cdot \boldsymbol{V} \\ \boldsymbol{\sigma} \cdot \boldsymbol{p} - \boldsymbol{\sigma} \cdot \boldsymbol{V} & -m + V - S - \omega \cdot J \end{pmatrix} \begin{pmatrix} f \\ g \end{pmatrix} = \varepsilon \begin{pmatrix} f \\ g \end{pmatrix}$$

$$S(\boldsymbol{r}) = \alpha_S \rho_S + \beta_V \rho_S^2 + \gamma_V \rho_S^3 + \delta_S \Delta\rho_S$$

$$V(\boldsymbol{r}) = \alpha_V \rho_V + \gamma_V \rho_V^3 + \delta_V \Delta\rho_V + \tau_3 \alpha_{TV} \rho_{TV} + \tau_3 \delta_{TV} \Delta\rho_{TV} + e\frac{1-\tau_3}{2} A$$

$$\boldsymbol{V}(\boldsymbol{r}) = \alpha_V \boldsymbol{j}_V + \gamma_V \boldsymbol{j}_V^3 + \delta_V \Delta\boldsymbol{j}_V + \tau_3 \alpha_{TV} \boldsymbol{j}_{TV} + \tau_3 \delta_{TV} \Delta\boldsymbol{j}_{TV} + e\frac{1-\tau_3}{2} \boldsymbol{A}$$

Consistent treatment for time-odd fields from nuclear currents

PWZ, Zhang, Peng, Liang, Ring, Meng, PLB 699, 181 (2011)

PWZ PLB 773, 1 (2017)

Applications of TAC-CDFT for chiral nuclei

$^{102\text{-}107}$Rh, ^{106}Ag, **^{135}Nd**, ^{136}Nd, $^{120\text{-}134}$Cs

PWZ PLB 773, 1-5 (2017)

PWZ, Wang, and Chen, PRC 99, 054319 (2019)

Peng and Chen, PLB 810, 135795 (2020)

Peng and Chen, PRC 105, 044318 (2022)

Chen, Li, and Guo, EPJA 59, 142 (2023)

D3-D4 $\pi[h^1_{11/2}(gd)^1] \otimes \nu h^{-1}_{11/2}$

D5-D6 $\pi h^2_{11/2} \otimes \nu h^{-1}_{11/2}$

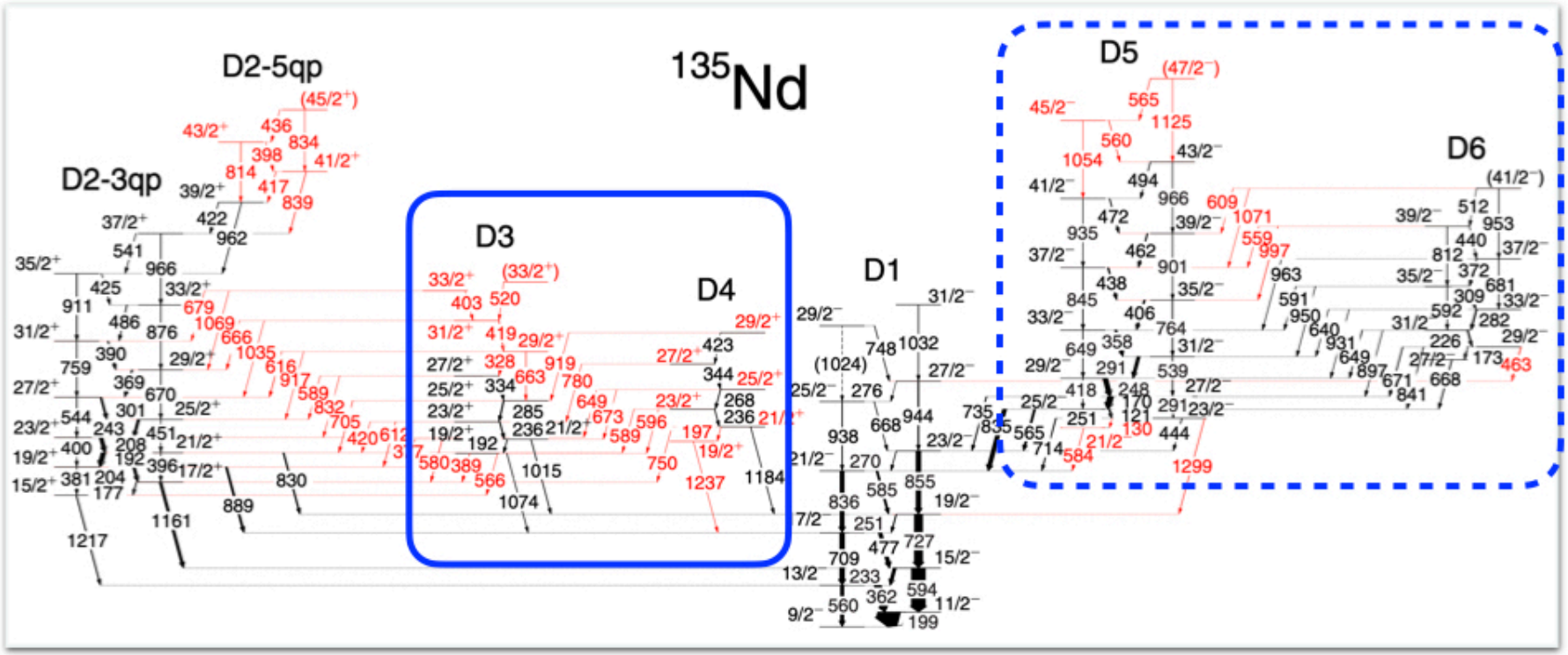

Experimental Data from Lv et al., Phys. Rev. C 100, 024314 (2019)

Energy surface against tilted angles

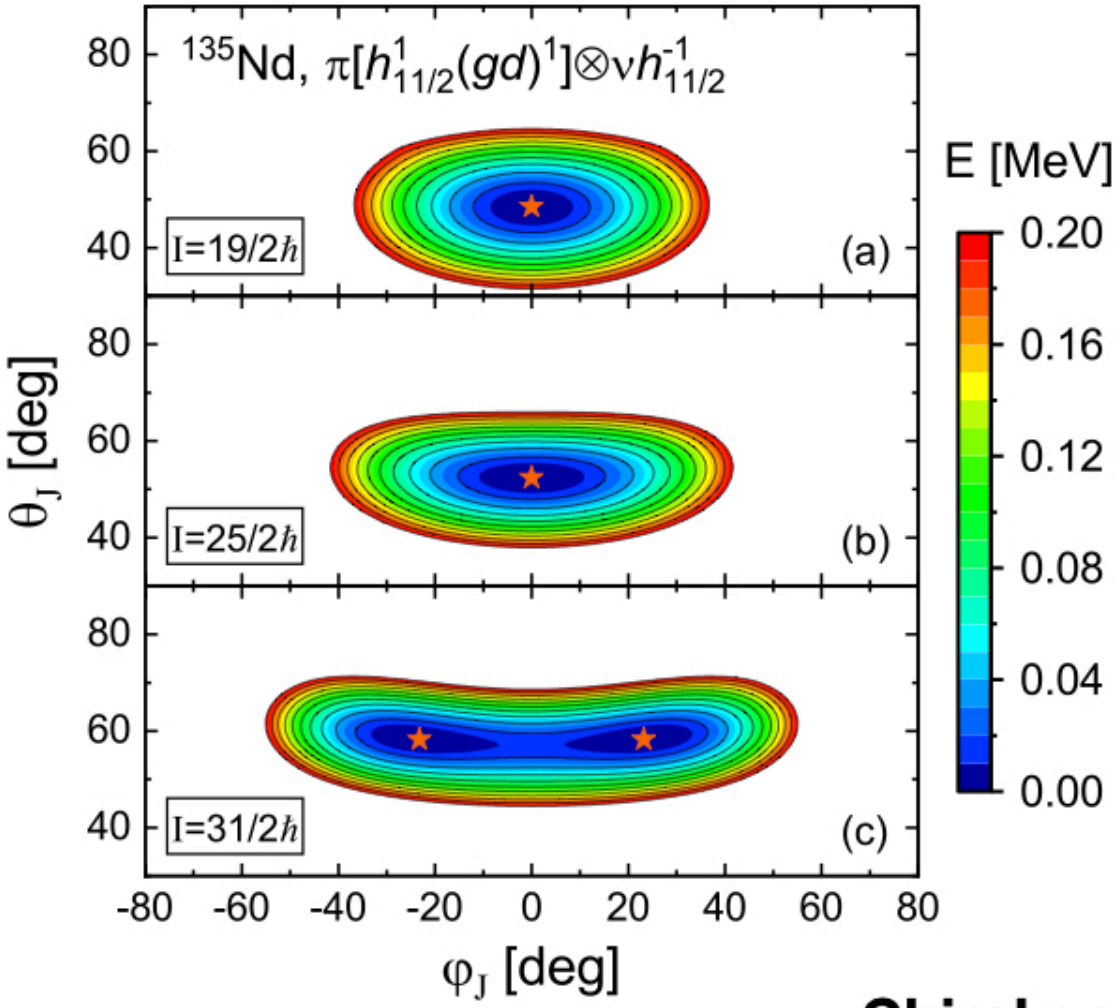

polar angle θ
azimuth angle φ

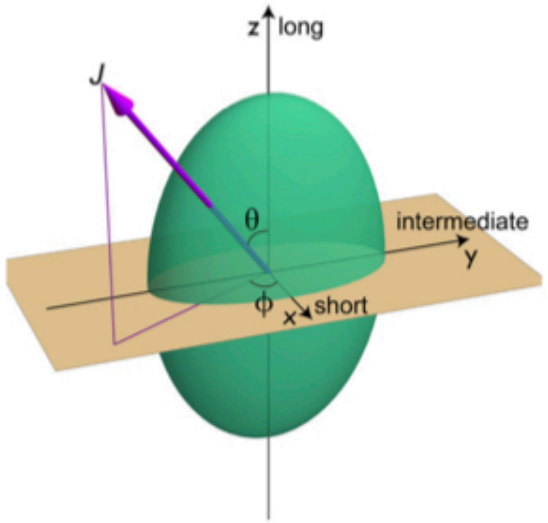

Chiral geometry is clearly seen.

Ren, PWZ, Meng, PRC, **105**, L011301 (2022)

Energy spectrum

The lower bands are well reproduced.

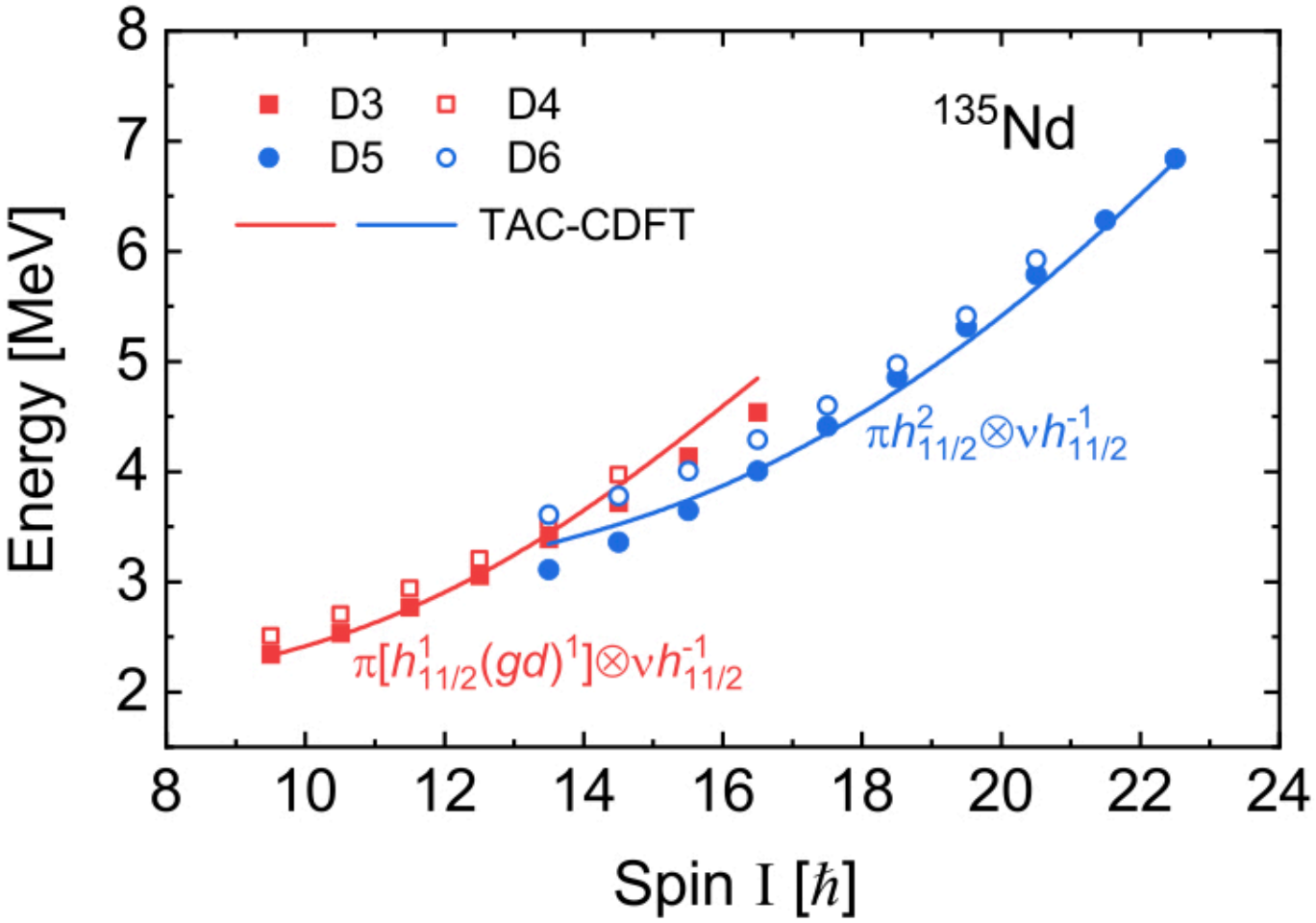

Ren, PWZ, Meng, PRC, **105**, L011301 (2022)

Time-dependent CDFT

The many-body problem is mapped onto a one-body problem!

Runge-Gross Theorem

There is a unique mapping between the time dependent external potential and the density, for many body systems evolving from a given initial state.

Runge and Gross, PRL 52, 997 (1984)

Time-dependent Kohn-Sham DFT

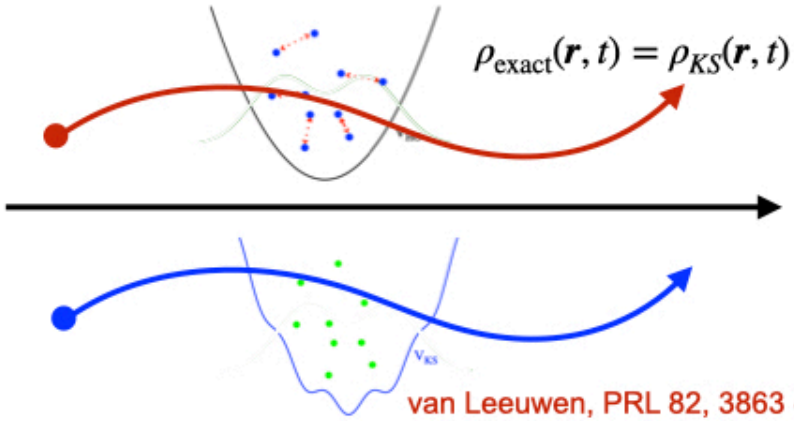

van Leeuwen, PRL 82, 3863 (1999)

Ren, PWZ, Meng, PLB 801,135194 (2020)

$$i\partial_t \begin{pmatrix} f \\ g \end{pmatrix} = \begin{pmatrix} m + V + S & \boldsymbol{\sigma}\cdot\boldsymbol{p} - \boldsymbol{\sigma}\cdot\boldsymbol{V} \\ \boldsymbol{\sigma}\cdot\boldsymbol{p} - \boldsymbol{\sigma}\cdot\boldsymbol{V} & -m + V - S \end{pmatrix} \begin{pmatrix} f \\ g \end{pmatrix}$$

$$\rho(\boldsymbol{r},t) = \sum_i^N f_i^2 + g_i^2$$

Applications of the TD-CDFT

3D Lattice: no spatial symmetry restriction

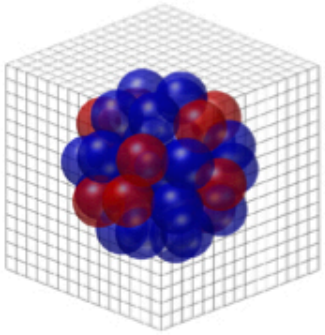

✓ Applications include:

- Linear alpha-chain — PRL 115, 022501 (2015) PLB 801,135194 (2020)
- Nuclear fission — PRL 128, 172501 (2022) PRC 105, 044313 (2022) PRC 107, 014303 (2023)
- Chiral dynamics — PRC 105, L011301 (2022)
- $^{16}O + {}^{16}O$ reaction — PRC 102, 044603 (2020)
- …

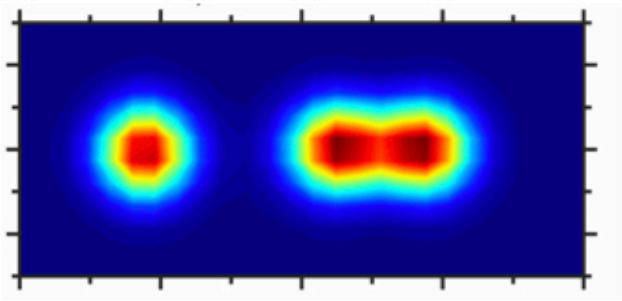

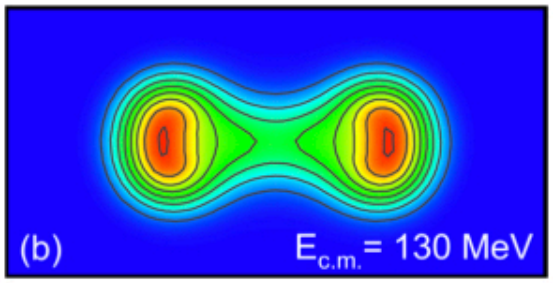

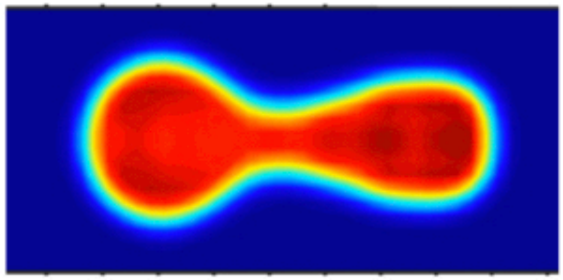

Chiral dynamics in triaxial nuclei

Chiral Precession across left and right sectors

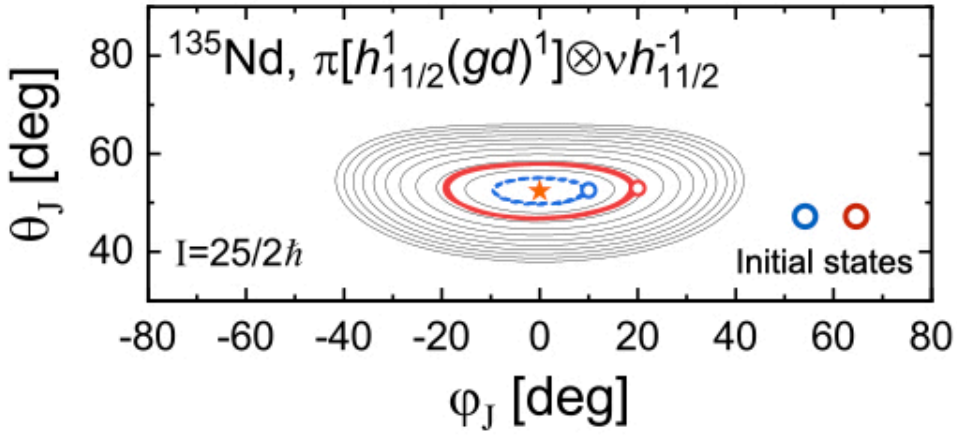

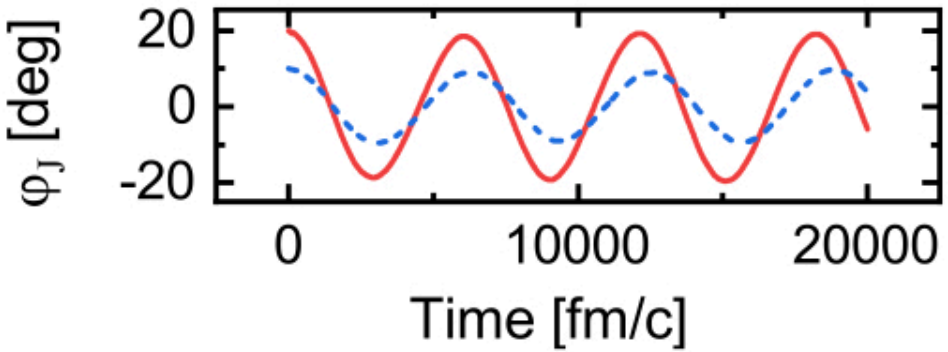

Precession periods are roughly **identical**.

Space-fixed frame

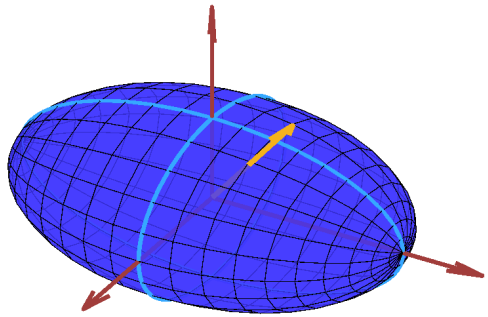

Body-fixed frame

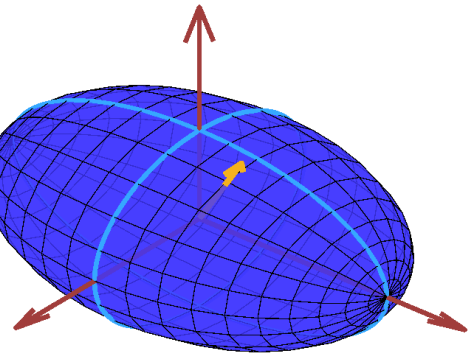

Ren, PWZ, Meng, PRC, **105**, L011301 (2022)

Chiral precession

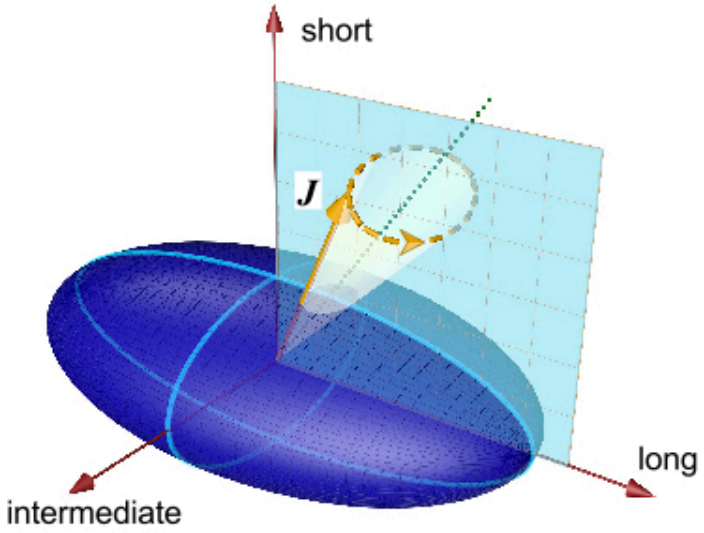

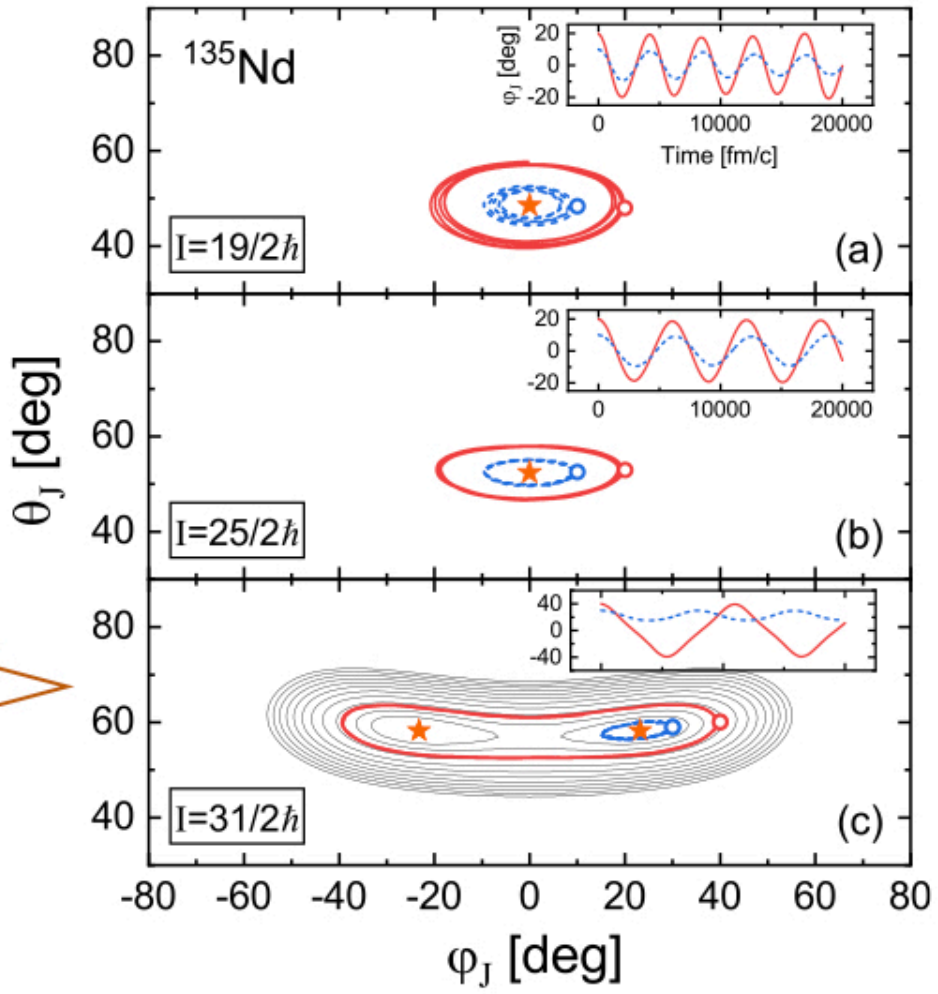

For 31/2 $\hbar$, trajectories are disparate not only in amplitudes but also in periods.

anharmonic effects, quantum tunneling; **requantization of the TD-CDFT**

Ren, PWZ, Meng, PRC, **105**, L011301 (2022)

Chiral excitation energies via Fourier analyses

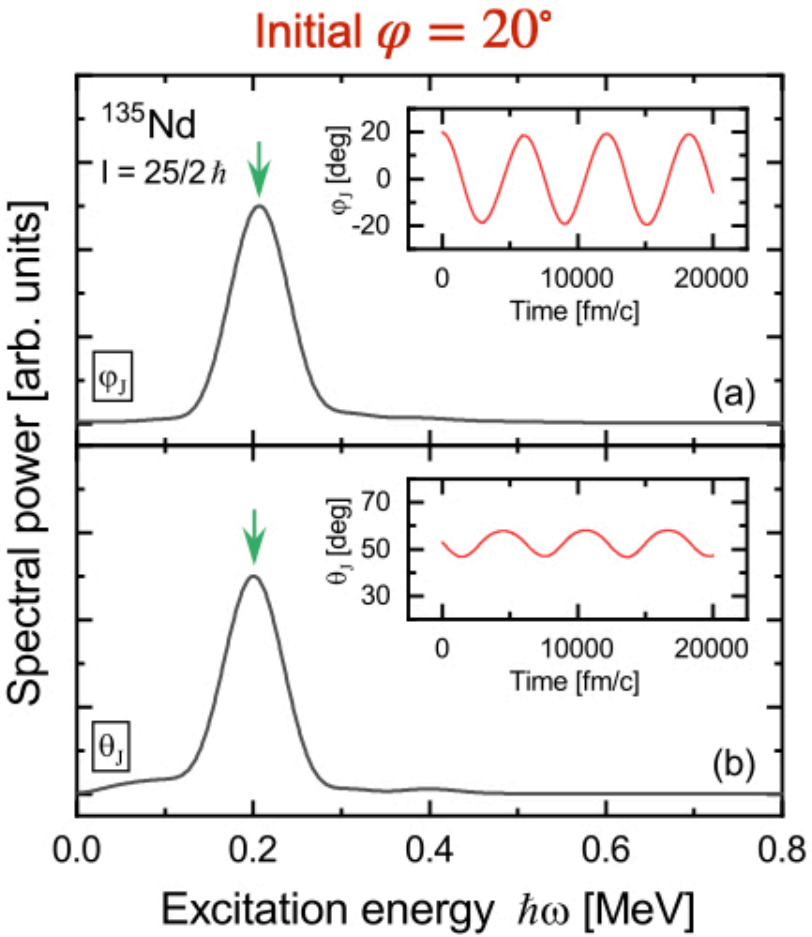

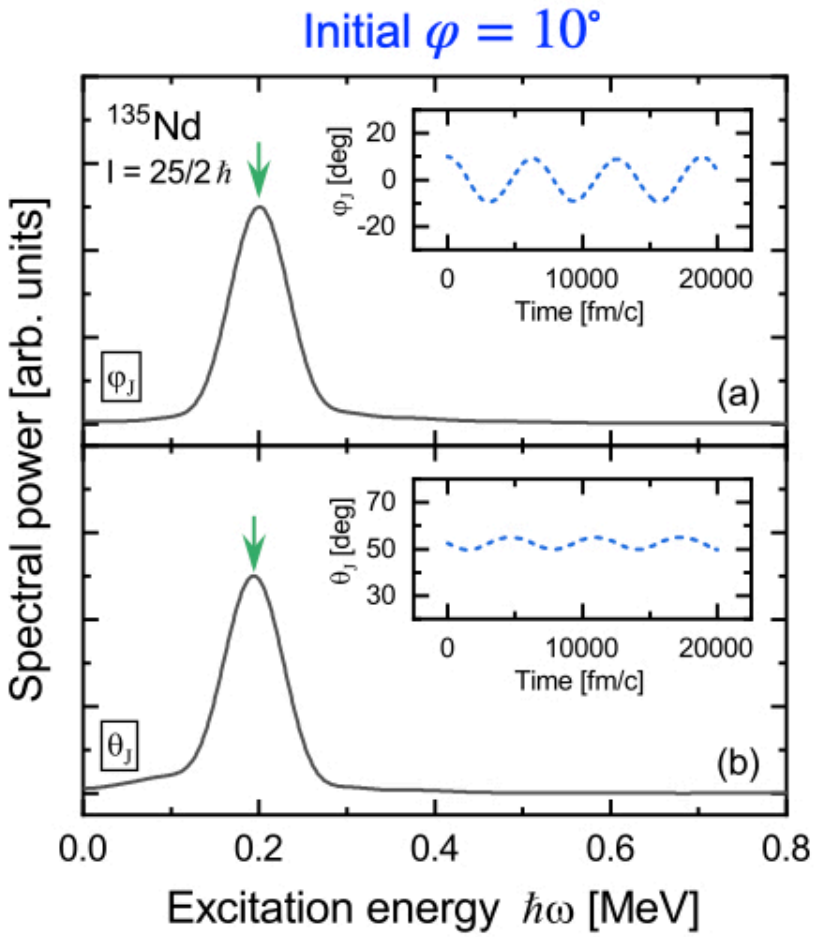

Ren, PWZ, Meng, PRC, **105**, L011301 (2022)

Energy spectrum

Ren, PWZ, Meng, PRC, **105**, L011301 (2022)

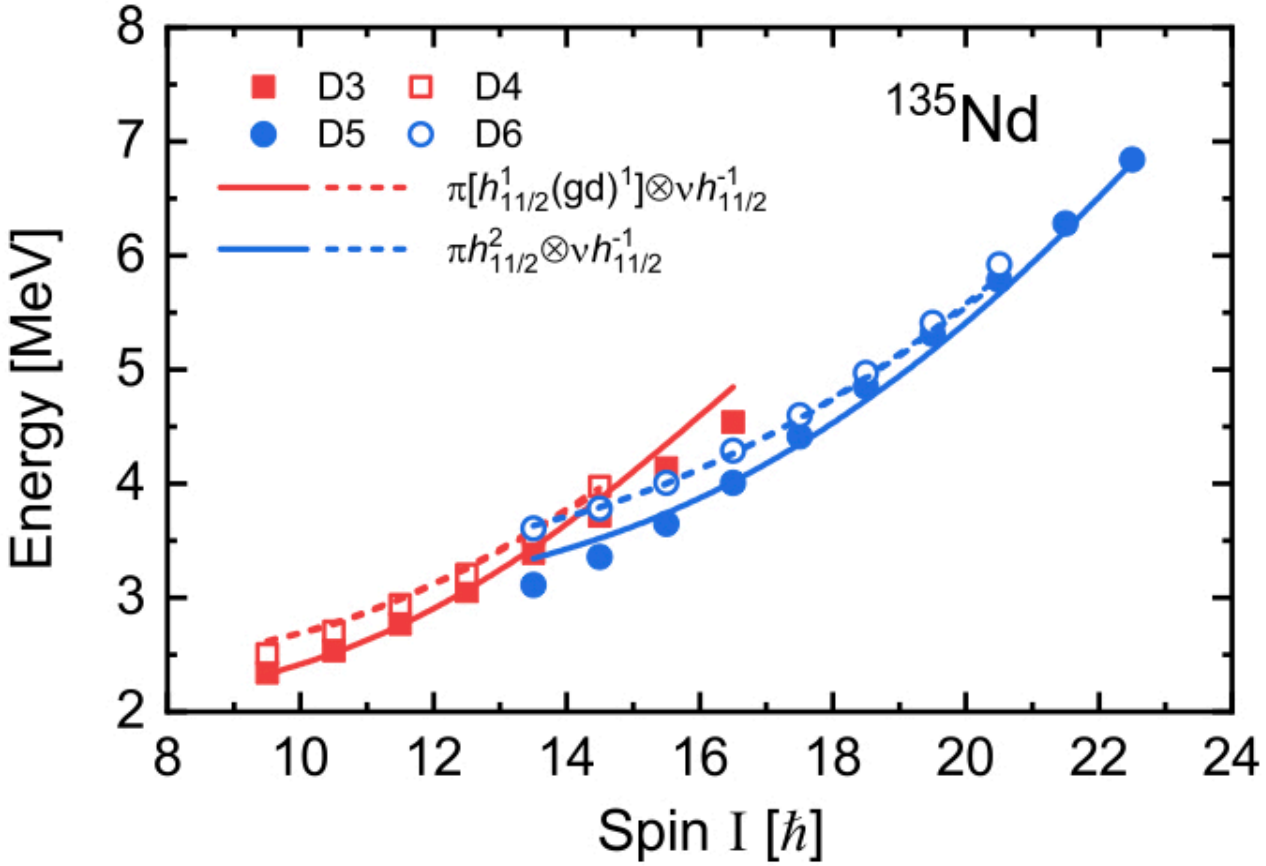

The first fully microscopic and self-consistent description for the ***chiral twin bands*** in the framework of DFTs.

Chiral conundrum in ^{106}Ag

PRL **98,** 102501 (2007) PHYSICAL REVIEW LETTERS week ending 9 MARCH 2007

Effect of γ Softness on the Stability of Chiral Geometry: Spectroscopy of ^{106}Ag

P. Joshi,[1] M. P. Carpenter,[2] D. B. Fossan,[3] T. Koike,[3,4] E. S. Paul,[5] G. Rainovski,[5,3,6] K. Starosta,[3,7] C. Vaman,[3,7] and R. Wadsworth[1]

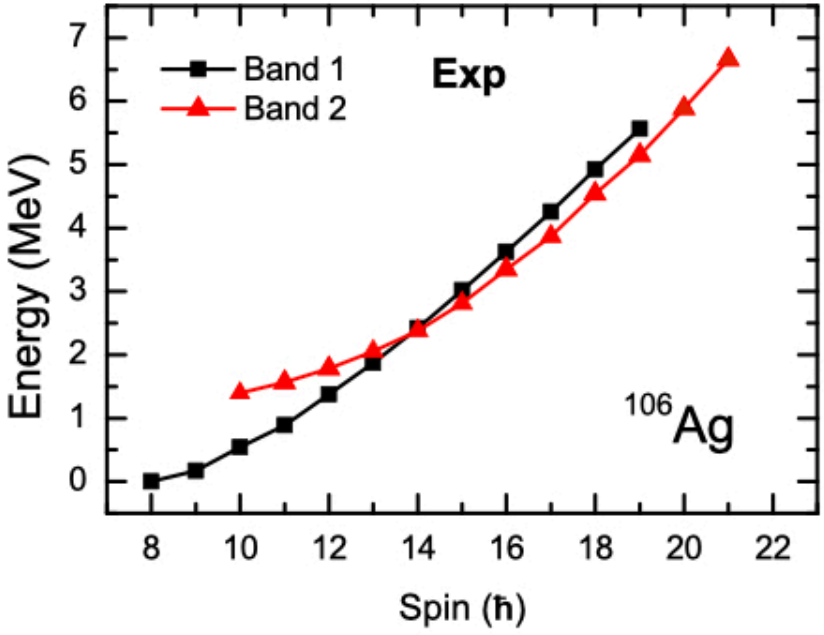

Chiral conundrum in ^{106}Ag

PRL **112,** 202503 (2014) PHYSICAL REVIEW LETTERS week ending 23 MAY 2014

Exploring the Origin of Nearly Degenerate Doublet Bands in ^{106}Ag

N. Rather,[1] P. Datta,[2,*] S. Cha
R. Palit,[4] S. I

PRL **112,** 202502 (2014) PHYSICAL REVIEW LETTERS week ending 23 MAY 2014

Resolution of Chiral Conundrum in ^{106}Ag: Doppler-Shift Lifetime Investigation

E. O. Lieder,[1,2] R. M. Lieder,[1,*] R. A. Bark,[1] Q. B. Chen,[3] S. Q. Zhang,[3] J. Meng,[3,4,5] E. A. Lawrie,[1] J. J. Lawrie,[1] S. P. Bvumbi,[1] N. Y. Kheswa,[1] S. S. Ntshangase,[1] T. E. Madiba,[1] P. L. Masiteng,[1] S. M. Mullins,[1] S. Murray,[1] P. Papka,[1] D. G. Roux,[6] O. Shirinda,[1] Z. H. Zhang,[3] P. W. Zhao,[3] Z. P. Li,[7] J. Peng,[8] B. Qi,[9] S. Y. Wang,[9] Z. G. Xiao,[10,11] and C. Xu[3]

Consistent data but different interpretation

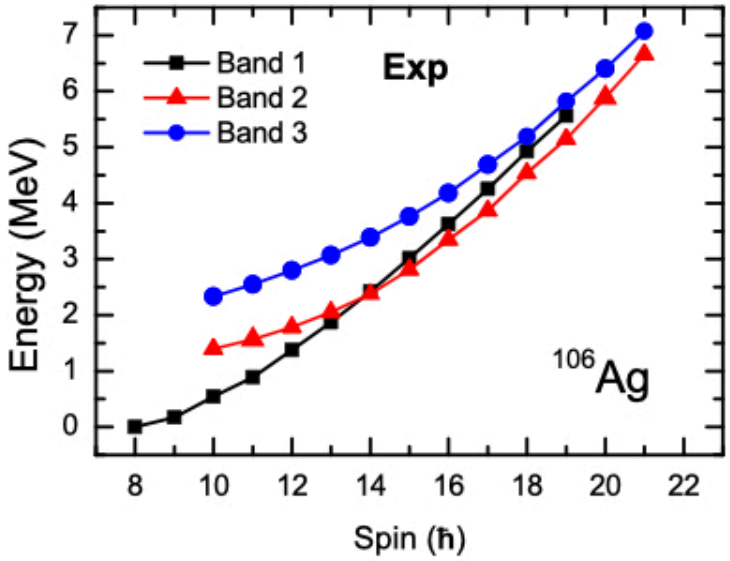

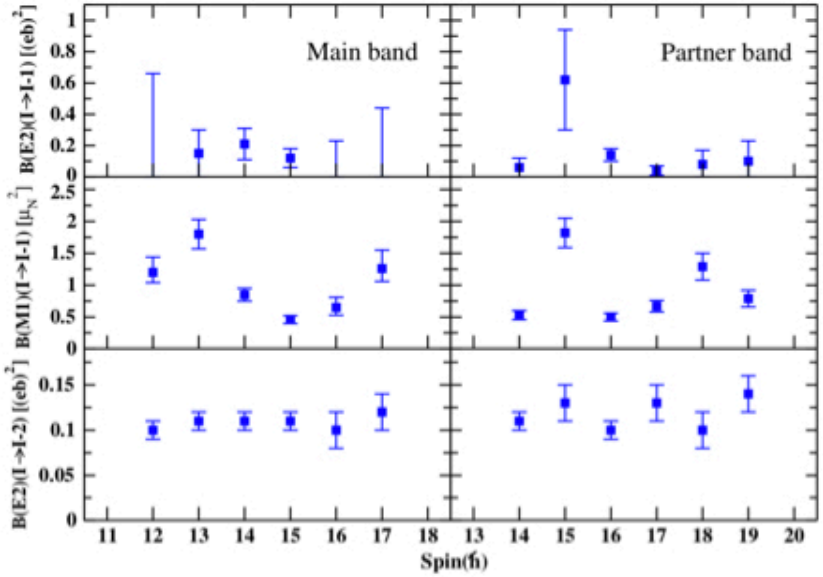

TAC-CDFT for chiral conundrum in ^{106}Ag

PWZ, Wang, Chen PRC 99, 54319 (2019)

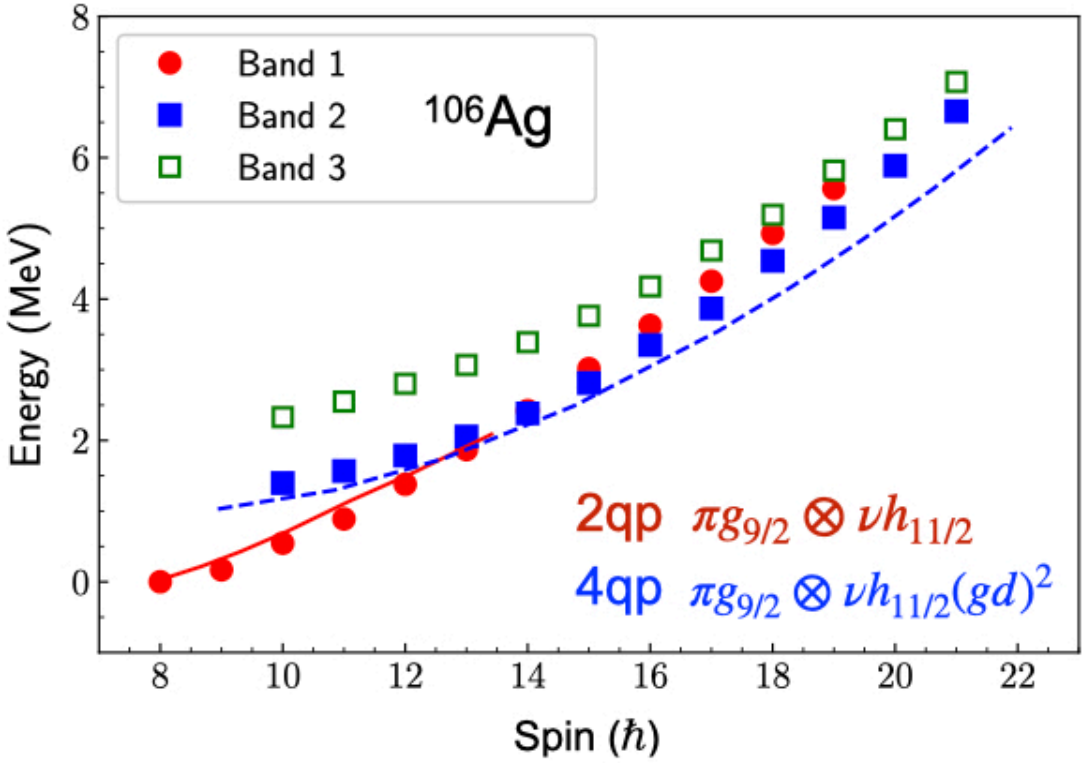

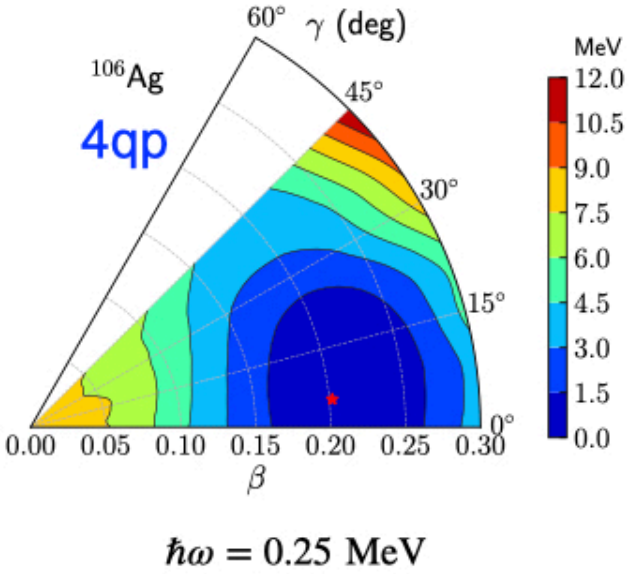

The energy for bands 1 and 2 are well reproduced with two distinct configurations.

For the 4qp configuration, the potential energy surface is rather soft against triaxiality.

Energy surface against tilted angles

PWZ, Wang, Chen PRC 99, 54319 (2019)

polar angle θ
azimuth angle φ

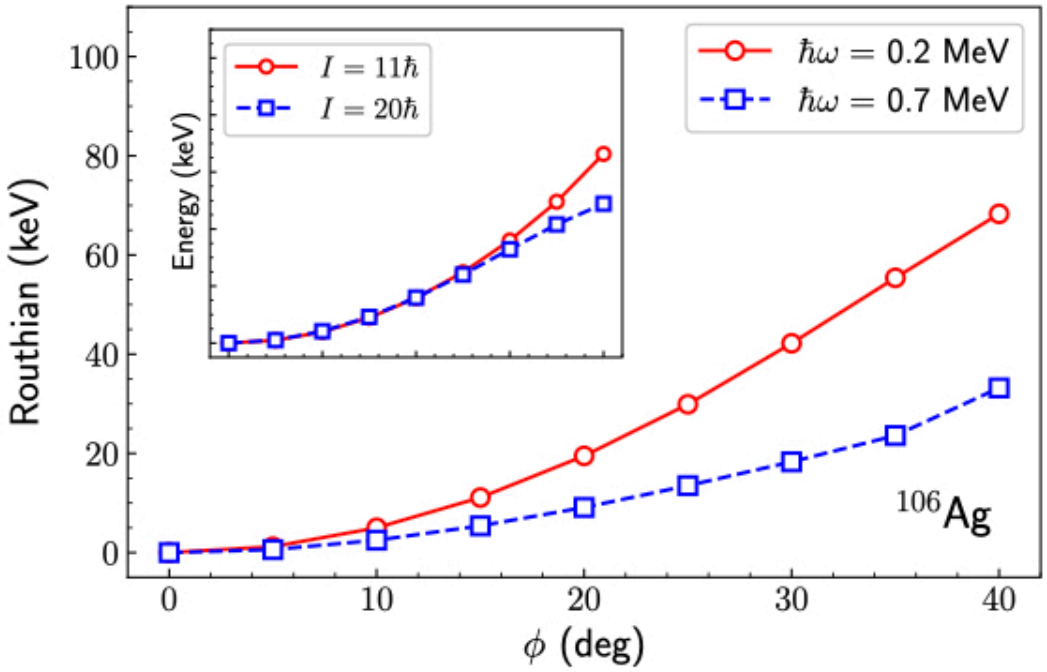

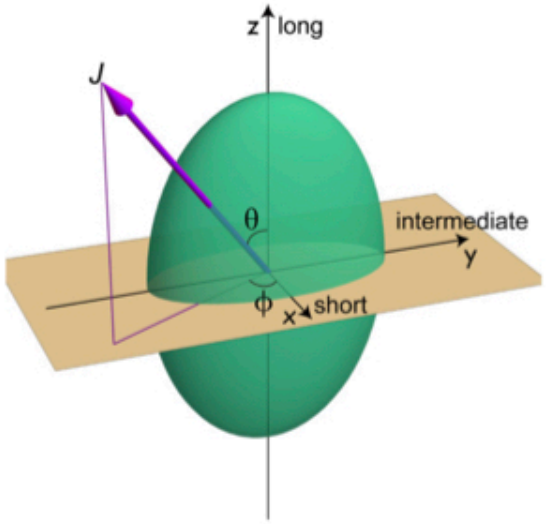

A chiral vibrational band could be expected due to the soft Routhian curves, which gives a possible explanation of band 3.

Chiral dynamics in ^{106}Ag

Chiral Precession couples Gamma Vibration

Li, et al., in preparation

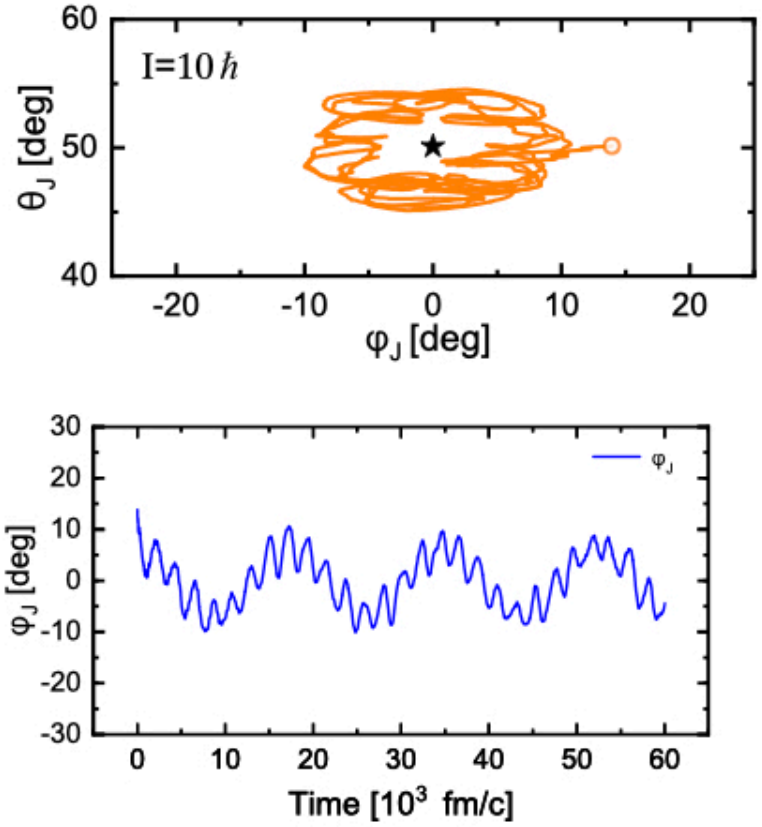

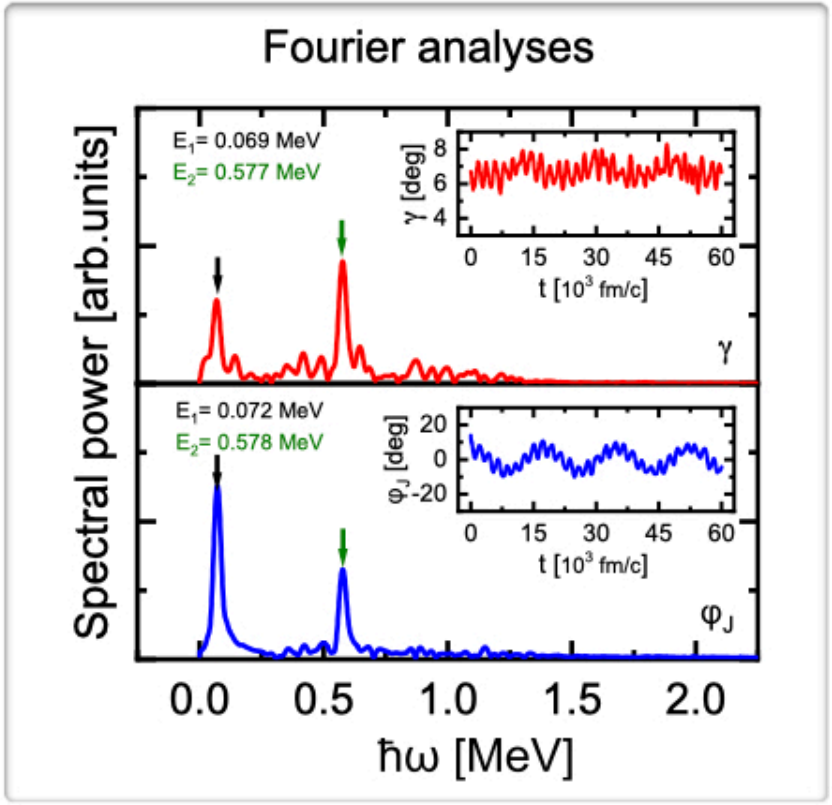

Two excitation modes can be extracted from the Phi and Gamma dynamics.

Chiral dynamics in ^{106}Ag

Chiral Precession couples Gamma Vibration

Li, et al., in preparation

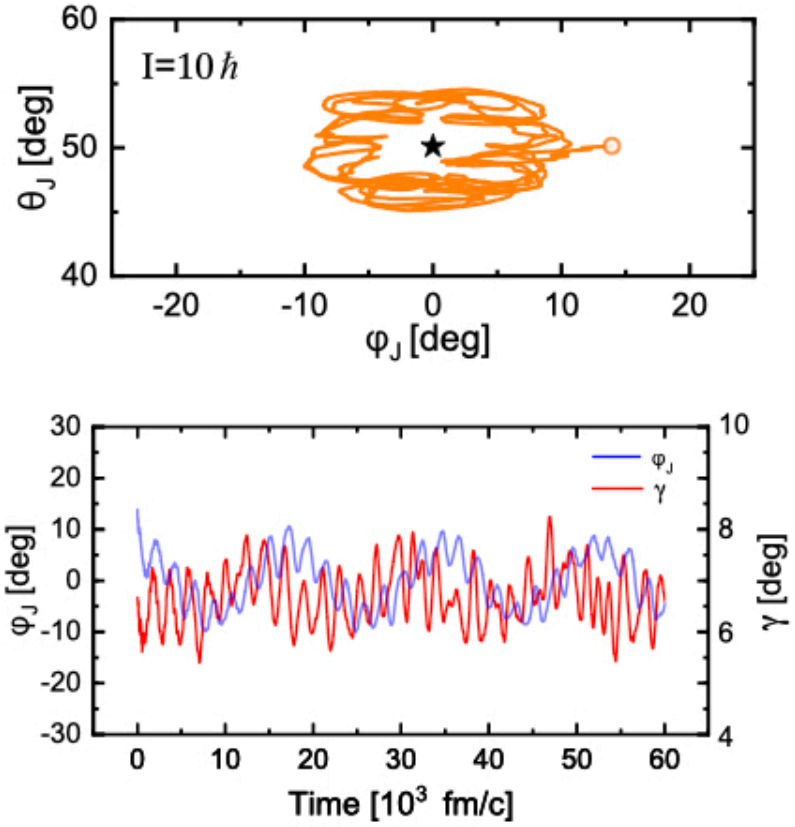

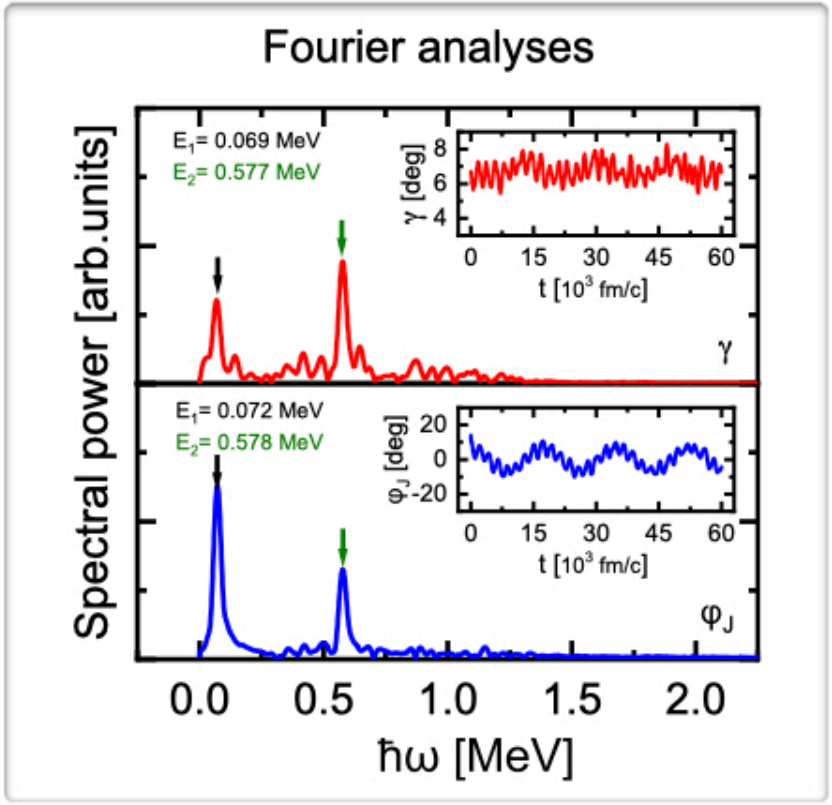

Two excitation modes can be extracted from the Phi and Gamma dynamics.

Chiral dynamics in ^{106}Ag

Chiral Precession couples Gamma Vibration

Li, et al., in preparation

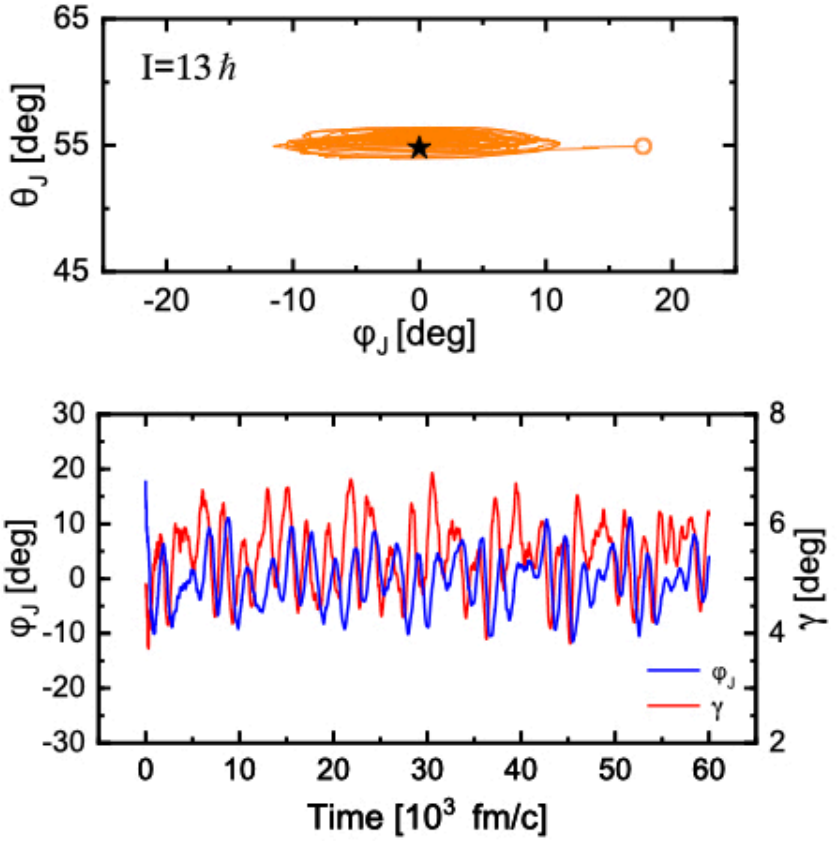

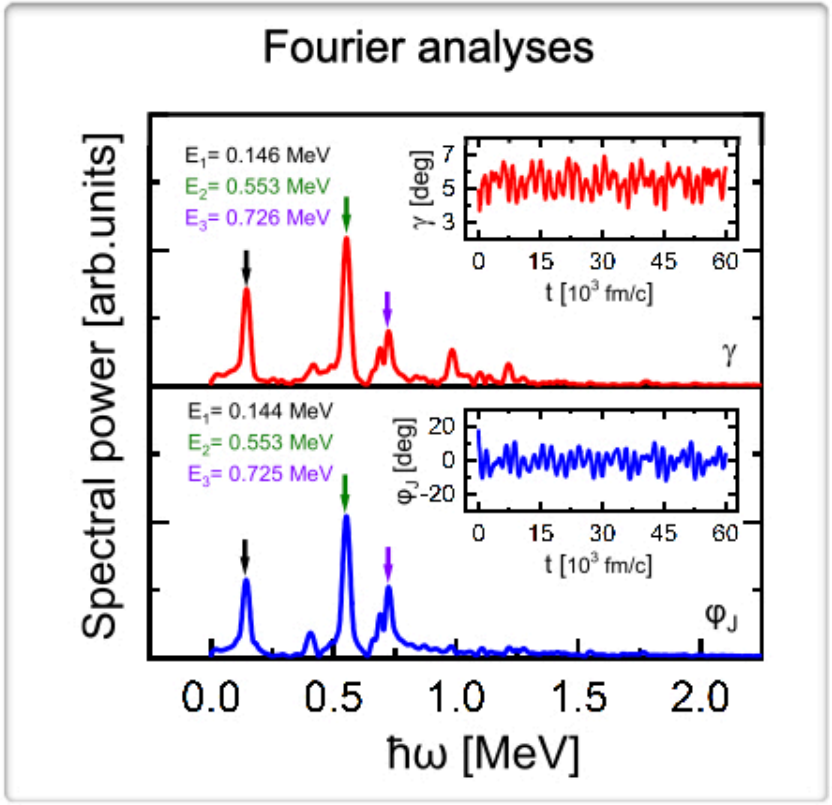

The two excitation modes are strongly coupled and the peak mainly associated with the gamma vibration are fragmented.

Chiral dynamics in ^{106}Ag

Chiral Precession couples Gamma Vibration

Li, et al., in preparation

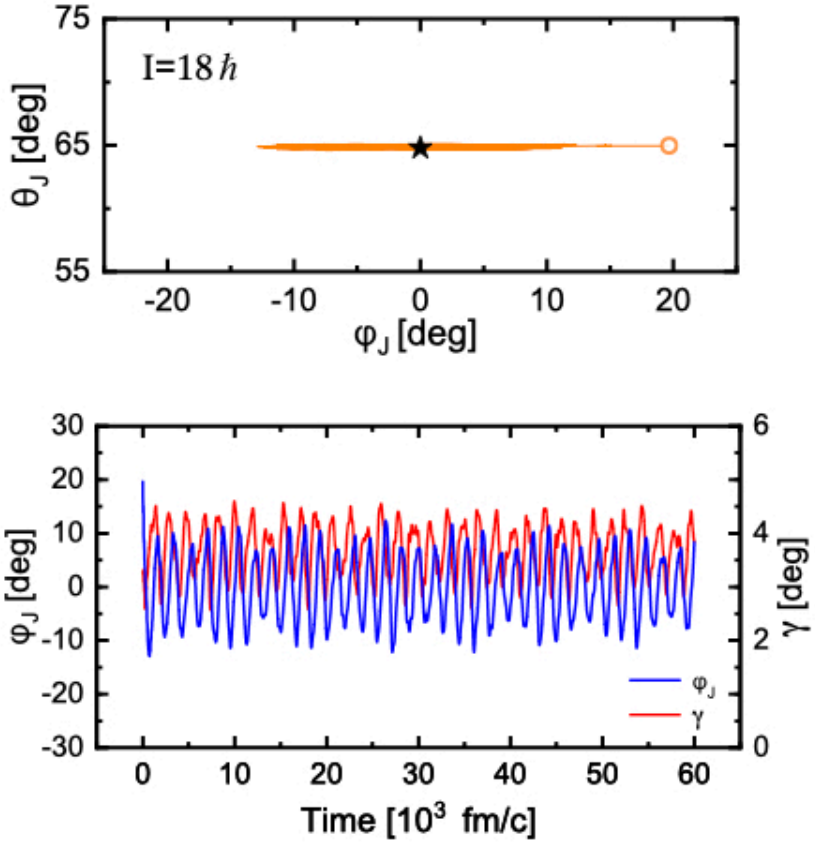

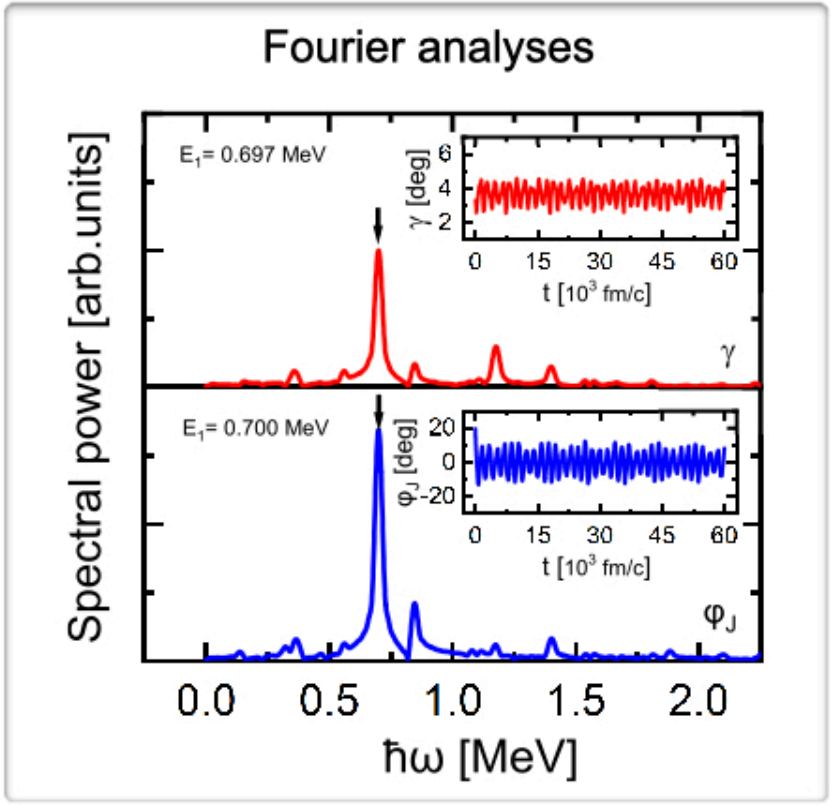

Gamma vibration is dominated, while chiral precession is suppressed.

Energy spectrum

Li, et al., in preparation

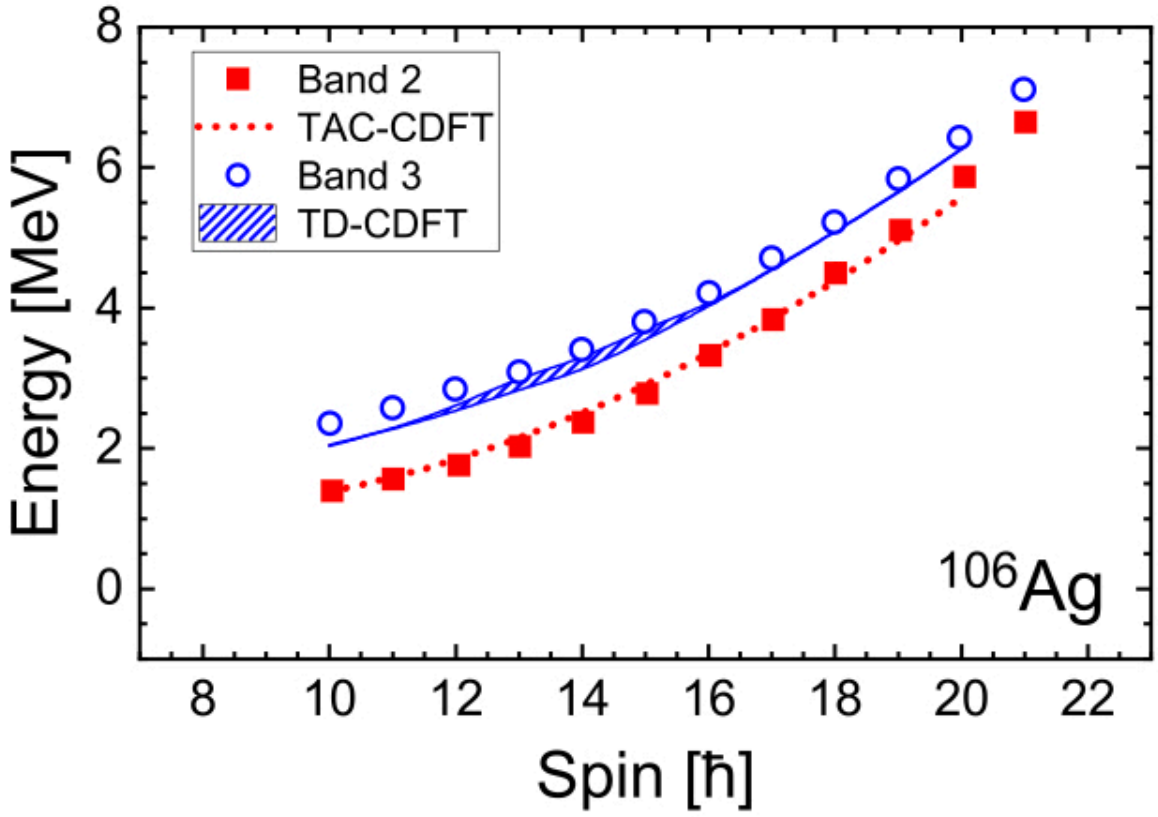

The chiral excitation energy is given by the sum of the two modes, i.e., the chiral precession and gamma vibration.

Summary

Covariant density functional theory has been improved and extended for a unified description of static and dynamic nuclear properties.

➢ **Chiral dynamics in triaxial nuclei**

✓ Static TAC-CDFT calculations

The lower band is well reproduced.

✓ Dynamic TD-CDFT calculations

The TAC-CDFT results are taken as the initial states.

The upper band is well reproduced.

✓ A novel mechanism, chiral precession, is revealed.

✓ The chiral dynamics and its interplay with the gamma vibration in gamma soft nuclei is explored.

Collaborations

Beijing
Jie Meng
Zhengxue Ren
Shuangquan Zhang

Chongqing
Zhipan Li

Munich
Peter Ring

and many experimental colleagues …

Thank you for your attention!

Chiral excitation energies from Fourier analyses

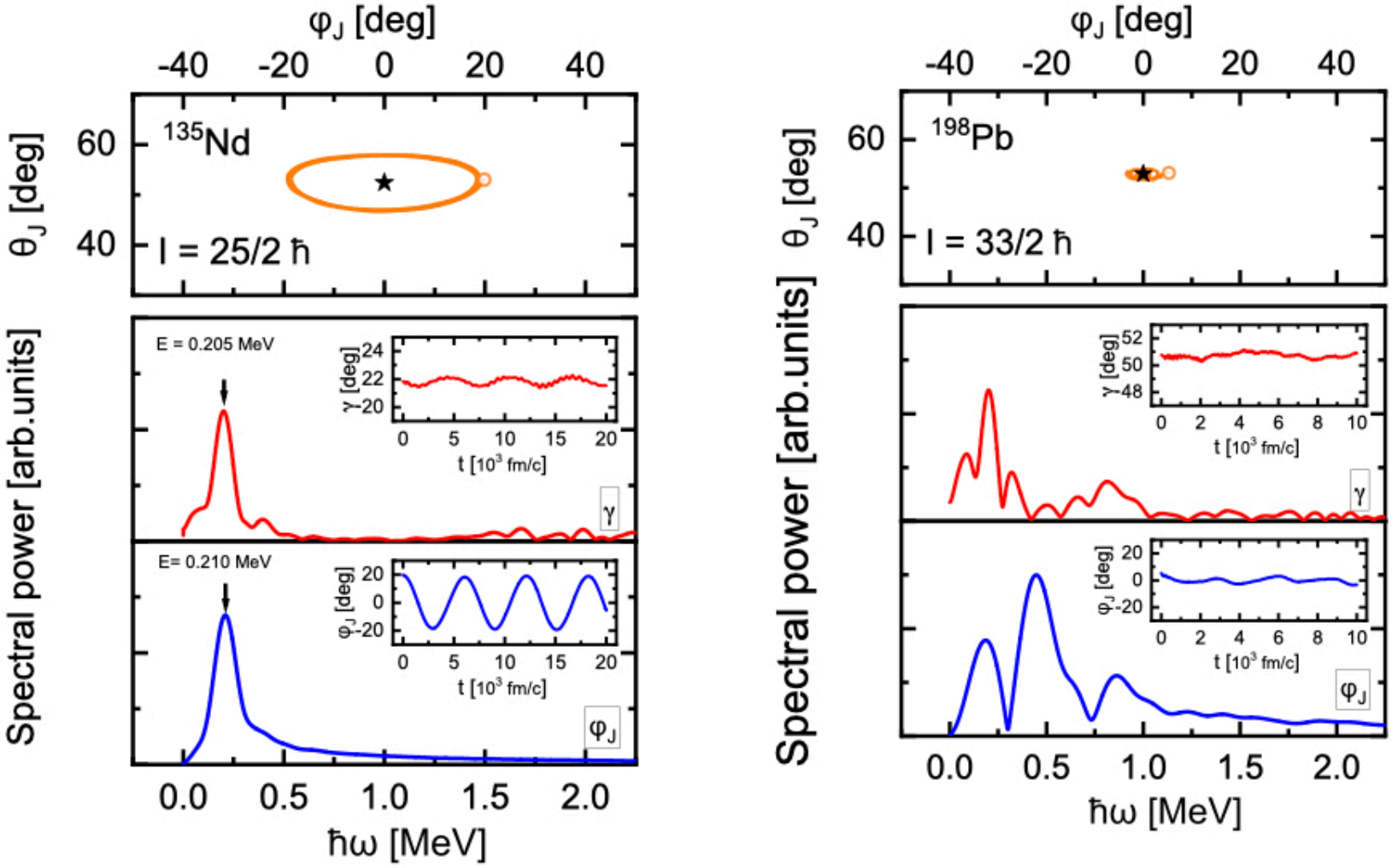

Ren, PWZ, Meng, PRC, **105**, L011301 (2022)

TAC-CDFT for chiral conundrum in ^{106}Ag

PWZ, Wang, Chen PRC 99, 54319 (2019)